Available online at www.sciencedirect.com
ScienceDirect
Trans. Nonferrous Met. Soc. China 26(2016) 2144−2151
Transactions of Nonferrous Metals Society of China
www.tnmsc.cn

Corrosion and discharge performance of Mg−9%Al−2.5%Pb alloy as anode for seawater activated battery

Min DENG, Ri-chu WANG, Yan FENG, Nai-guang WANG, Lin-qian WANG

School of Materials Science and Engineering, Central South University, Changsha 410083, China

Received 5 September 2015; accepted 22 March 2016

Abstract: To obtain a new kind of Mg−Al−Pb alloy anode material with low content of Pb, the corrosion and discharge behavior of Mg−9%Al−2.5%Pb (hereafter in mass fraction) alloy were investigated by immersion tests and electrochemical techniques, and compared with those of Mg−6%Al−5%Pb alloy. The results indicate that Mg−9%Al−2.5%Pb alloy exhibits a lower self-corrosion rate and higher utilization efficiency in contrast with Mg−6%Al−5%Pb alloy because of the higher content of Al. As the result of the decrease of Pb content, the discharge activity of Mg−9%Al−2.5%Pb alloy is relatively weaker but still meets the requirement of anode. These results reveal that Mg−9%Al−2.5%Pb alloy with a low content of Pb can serve as a good candidate for the anode material used in seawater activated battery.

Key words: Mg−Al−Pb alloy; anode material; self-corrosion rate; utilization efficiency; discharge activity

1 Introduction

Seawater activated battery is a kind of power source which utilizes seawater as the electrolyte [1,2], leading to a distinct mass reduction of the battery system. Thus, seawater activated battery usually exhibits significantly higher energy density than other batteries [3,4]. This battery serves as candidate for a wide range of underwater applications, e.g., lifebuoys, sonobuoys, torpedoes, life raft, and detection devices [5,6]. Because of its wide application, seawater activated battery has been emphasized and researched in many countries recently.

The generation of the electrochemical potential of seawater activated battery relies on the corrosion of a reactive anode metal in electrolyte (seawater) and the reduction of the metal chloride cathode [7]. The discharge performance of seawater activated battery is principally determined by the anode, which plays a vital role in enhancing the cell voltage and inhibiting the self-discharge [8]. Thus, it is of crucial importance to use proper metals to serve as anodes for seawater activated batteries. Magnesium is an attractive anode material in such battery because its several advantages, for example, negative electrode potential of −2.73 V (vs standard hydrogen electrode (SHE)), high Faradic capacity of 2.2 A·h/g, and low density of 1.74 g/cm^3 [9−11]. However, there are several issues that will adversely affect its performance when this metal is used for practical application. Firstly, the corrosion resistance of magnesium is not well enough. It is prone to suffering self-discharge or side hydrogen evolution reaction in seawater electrolyte, signifying that the metal cannot be completely used to generate current and the anode utilization efficiency will decrease [12]. Secondly, the electrode surface of magnesium is usually covered by a $Mg(OH)_2$ film [13], which will reduce the reaction surface area and therefore debase its discharge performance.

To enhance the corrosion and discharge performance of magnesium anodes, a common approach is to dope magnesium with other alloying elements [14]. In the past few years, several magnesium alloy anodes have been developed for military and commercial applications. Typically, AP65 alloy with a nominal composition of Mg−6%Al−5%Pb, which is developed by British Magnesium Electronics Company and has been used in electric torpedo [15], is one of the magnesium alloy anodes. Unfortunately, lead with

Foundation item: Projects (51401243, 51101171) supported by the National Natural Science Foundation of China; Projects (2015T80883, 2014M552151) supported by China Postdoctoral Science Foundation
Corresponding author: Yan FENG; Tel: +86-13755199741; E-mail: fengyanmse@csu.edu.cn
DOI: 10.1016/S1003-6326(16)64330-3

toxicity is not environment friendly. Thus, in this work, we investigate the corrosion and discharge behaviors of Mg−9%Al−2.5%Pb alloy in 3.5%NaCl solution, and compare its electrochemical performance with that of AP65 magnesium alloy. The aim of this work is to reduce the content of lead in AP65 but sustain its desirable discharge and corrosion performance.

2 Experimental

Mg−6%Al−5%Pb and Mg−9%Al−2.5%Pb alloys were prepared by melting the ingots of high purity magnesium (99.99%), aluminum (99.99%), lead (99.99%) in a resistance furnace at 720 °C. The molten metal was then poured into a water-cooled steel mold with the protection of sulfur powder. The actual compositions of the two alloys were examined with inductively coupled plasma atomic emission spectrometry (ICP-AES); the data indicated that the relative deviation for the content of each element was less than ±5% while the content of each impurity was lower than 0.1%. The phase structures of this two alloys were identified with an X-ray diffraction meter (XRD). The microstructures of the alloys were observed with a Quanta−200 scanning electron microscope (SEM) using backscattered electron (BSE) image.

The specimens of Mg−6%Al−5%Pb and Mg−9%Al−2.5%Pb alloys were prepared for electrochemical tests to study their discharge behavior. Each specimen was polished with 1000 grit SiC abrasive paper and exposed to 3.5% NaCl solution with a surface of 10 mm × 10 mm. The 3.5% NaCl solution made with analytical grade NaCl and distilled water was used to simulate seawater [9,10]. The electrochemical tests were carried out at room temperature using an IM6ex potentiostat/galvanostat system equipped with a three-electrode glass cell. The working and counter electrodes were experimental alloys and platinum plate, respectively. The saturated calomel electrode (SCE) served as the reference electrode.

The potentiodynamic polarization curves were obtained by sweeping the potential from −2.1 to −1.2 V (vs SCE) at a scan rate of 1 mV/s. The galvanostatic potential−time curves were recorded at the impressed anodic current densities of 10 or 180 mA/cm^2 for 600 s. The corroded surfaces after galvanostatic discharge were observed with the Quanta−200 SEM using secondary electron (SE) image. The utilization efficiencies of the magnesium anodes during galvanostatic discharge at 180 mA/cm^2 for 1 h were measured by mass loss method with chromic acid to remove the corrosion products. The utilization efficiency was then calculated according to the following relation [16]:

$$\eta = \frac{m_t}{m_a} \times 100\% \quad (1)$$

where η is the utilization efficiency (%), m_t is the theoretical mass loss (g) corresponding to the impressed current, and m_a is the actual mass loss (g) during the discharge period. The theoretical mass loss was calculated using the equation [16]:

$$m_t = \frac{It}{F\sum(\frac{f_i n_i}{a_i})} \quad (2)$$

where I is the impressed current (A); t is the discharge time (s); F is the Faraday constant (96485 C/mol); f_i, n_i and a_i are the mass fraction, ionic valence, and molar mass (g/mol) of the element, respectively. After the discharge tests, chromic acid was used to remove the discharge products to obtain the actual mass loss within the discharge period. Finally, the surface morphologies of the working electrodes after removing the discharge products were observed with a Quanta−200 SEM using secondary electron (SE) image.

The corrosion behavior was also evaluated using immersion tests in 3.5% NaCl aqueous solution at room temperature. The specimens were encapsulated in epoxy resin so that the surface with dimensions of 10 mm × 10 mm was exposed to the solution. The working surface was mechanically ground to 1000 grit SiC abrasive paper. The hydrogen evolved during the corrosion experiment was collected in a burette above the corroding sample and the volume of hydrogen was recorded for each hour. The evolved hydrogen is a direct measure of the corrosion rate [17,18] in the overall magnesium corrosion reaction:

$$Mg+H^+ + H_2O = Mg^{2+} + OH^- + H_2 \quad (3)$$

One molecule of hydrogen is evolved for each atom of corroded magnesium. The mass loss after immersion test was obtained after removing the corrosion products using chromic acid cleaning solution.

3 Results and discussion

3.1 Microstructure

Figure 1 shows the XRD analysis of Mg−6%Al−5%Pb and Mg−9%Al−2.5%Pb alloys. It reveals that the microstructures of the two different alloys both consist of two phases, i.e., the matrix α-Mg and β-$Mg_{17}Al_{12}$ phase. The addition of lead does not produce any compound with aluminum or magnesium, since lead has large solubility in magnesium (45% at 195 °C) and it mainly exists in the α-Mg matrix in the form of solid solution. Figure 2 presents the backscattered electron (BSE) images of Mg−6%Al−5%Pb and Mg−9%Al−2.5%Pb alloys. As shown in Figs. 2(a) and (c), the β-$Mg_{17}Al_{12}$

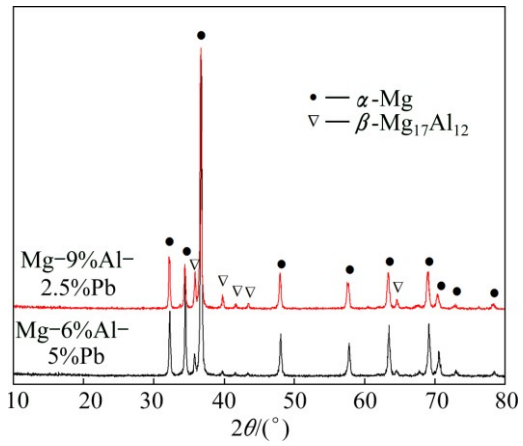

Fig. 1 XRD patterns for Mg−6%Al−5%Pb and Mg−9%Al−2.5%Pb alloys

phase mainly distributes at the grain boundaries. The amount of β-$Mg_{17}Al_{12}$ phase in Mg−9%Al−2.5%Pb alloy is more than that in Mg−6%Al−5%Pb alloy, attributed to the higher content of Al in Mg−9%Al−2.5%Pb alloy. It may be confirmed by the diffraction peak of β-$Mg_{17}Al_{12}$ in the XRD patterns shown in Fig. 1. As indicated in Figs. 2(b) and (d), the primary α-Mg phase is surrounded by the β-$Mg_{17}Al_{12}$ phase and eutectic magnesium phase (eutectic α+β phase) [19,20]. The formation of this microstructure is due to the massive primary crystal of α-Mg phase and meager eutectic phase. During the eutectic transformation, the eutectic α phase is attached to the primary α phase, while the other phase exists at the grain boundaries of the primary crystal alone. This kind of separated eutectic structure is so-called divorced eutectic. During the process of casting, the high cooling rate obtained from the water-cooled steel mold is beneficial to the formation of this kind of microstructure [21].

3.2 Potentiodynamic polarization

The polarization curves of the two alloys are shown in Fig. 3, and the corrosion parameters derived from these polarization curves are listed in Table 1. It is obvious that the electrochemical processes of the two alloys are mainly activation-controlled without passivation. Evolution of hydrogen is the dominant feature of the cathodic branch when the potential is more negative than the corrosion potential, whereas the metal oxidation occurs in the anodic branch when the potential is more positive than the corrosion potential [22]. According to Table 1, the corrosion potential of Mg−9%Al−2.5%Pb alloy is more positive than that of

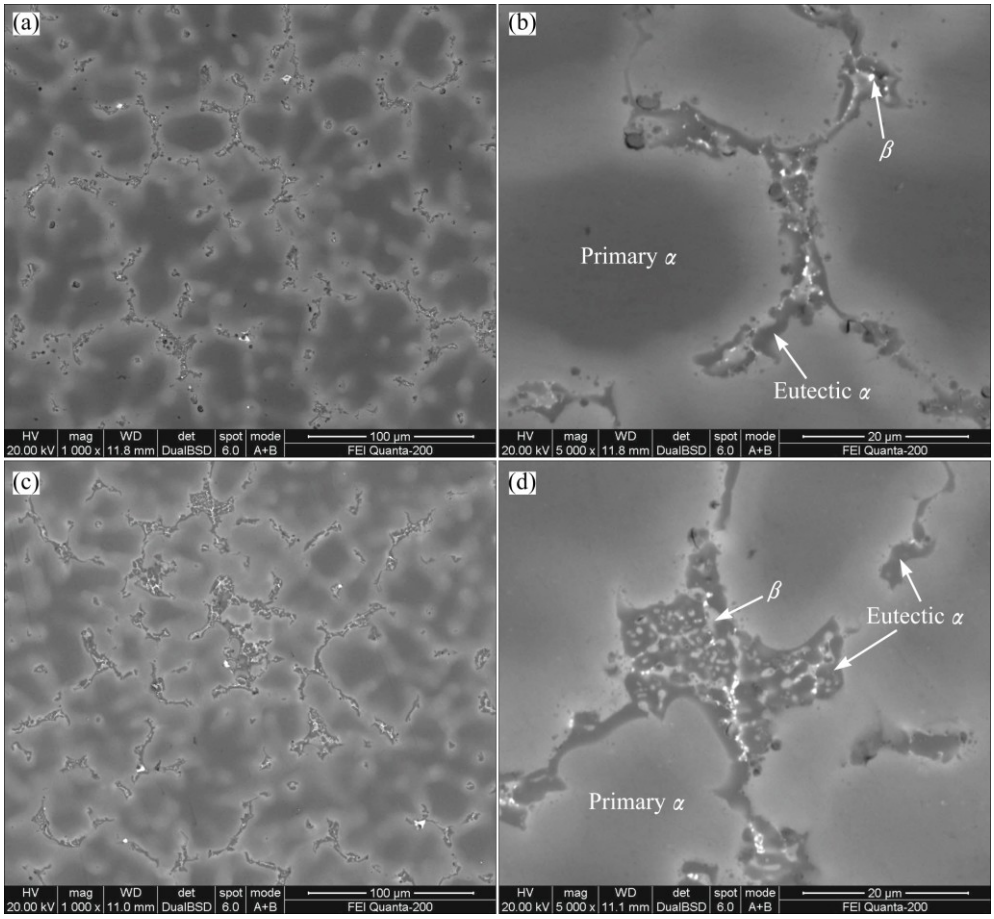

Fig. 2 Backscattered electron (BSE) images of Mg−6%Al−5%Pb (a, b) and Mg−9%Al−2.5%Pb (c, d)

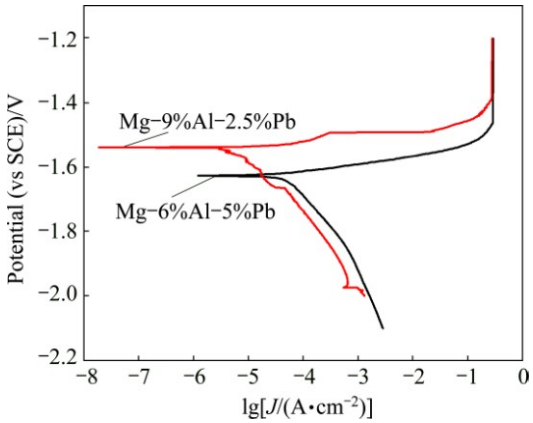

Fig. 3 Polarization curves of Mg−6%Al−5%Pb and Mg−9%Al−2.5%Pb alloys in 3.5% NaCl solution

Table 1 Corrosion parameters derived from polarization curves

Alloy	φ_{corr}(vs SCE)/V	J_{corr}/ (μA·cm^{-2})	b_c/ (mV·dec^{-1})
Mg−6%Al−5%Pb	−1.626	61.1±4.6	−177.2
Mg−9%Al−2.5%Pb	−1.538	11.2±2.3	−151.4

Mg−6%Al−5%Pb alloy. Meanwhile, the cathodic Tafel slope (b_c) of the two alloys is found to be different, indicating different hydrogen evolution behavior. The corrosion current densities listed in Table 1 are obtained by extrapolating the cathodic branches back to the corrosion potentials. The potential range used in extrapolating is more negative than corrosion potential by 125 to 250 mV. The corrosion current densities and the corresponding errors are the average values and the standard deviations of three parallel tests. It can be seen that the corrosion current density of Mg−9%Al−2.5%Pb alloy is smaller than that of Mg−6%Al−5%Pb alloy, indicating that the corrosion rate of Mg−9%Al−2.5%Pb alloy is lower.

3.3 Galvanostatic discharge

Figure 4 presents the galvanostatic potential−time curves of Mg−6%Al−5%Pb alloy and Mg−9%Al−2.5%Pb alloy at different current densities. The average discharge potentials of the two alloys are summarized in Table 2. In this work, a small current density of 10 mA/cm^2 is used to investigate the discharge behavior of magnesium alloy serving as the anode for long-term low-power applications, while a large current density of 180 mA/cm^2 is selected to evaluate the discharge performance of the anode materials used in high-power battery system [4,6]. It can be seen that the average discharge potentials of Mg−9%Al−2.5%Pb alloy at different current densities are slightly more positive than those of Mg−6%Al−5%Pb alloy. This signifies that the discharge activity of Mg−9%Al−2.5%Pb alloy is slightly weaker than Mg−6%Al−5%Pb alloy but the deviation is not obvious. In other words, Mg−9%Al−2.5%Pb alloy can also serve as a good candidate for the anode material used in seawater activated battery.

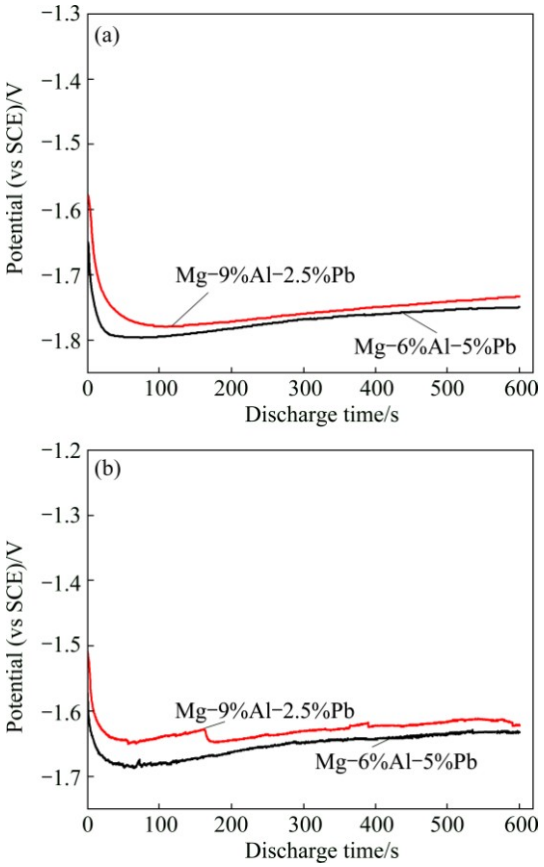

Fig. 4 Galvanostatic potential−time curves of different alloys in 3.5% NaCl solution at different anodic current densities: (a) 10 mA/cm^2; (b) 180 mA/cm^2

Table 2 Average discharge potentials of Mg−6%Al−5%Pb and Mg−9%Al−2.5%Pb alloys at different current densities for 600 s in 3.5% NaCl solution

Alloy	Average discharge potential (vs SCE)/V	
	10 mA/cm^2	180 mA/cm^2
Mg−6%Al−5%Pb	−1.770	−1.653
Mg−9%Al−2.5%Pb	−1.754	−1.628

The decline of discharge activity can be explained by the reduction of lead content. In Mg−Al−Pb alloy, aluminum and lead have synergistic reaction, while the lead is beneficial to the shedding of the corrosion products [23]. It is proved by the surface morphologies of the two alloys after discharging at 180 mA/cm^2 for 600 s as shown in Fig. 5. According to Figs. 5(a) and (b), the discharge products of Mg−6%Al−5%Pb alloy appear as the soil with many cracks, whereas the discharge products of Mg−9%Al−2.5%Pb alloy present as large and dense micro-blocks on the electrode surface. Therefore, during the discharge process, the electrolyte is

harder to penetrate through to effectively contact with the electrode surface of Mg−9%Al−2.5%Pb alloy, leading to a smaller active electrode area. That is why the reduction of lead content weakens the discharge activity of Mg−9%Al−2.5%Pb.

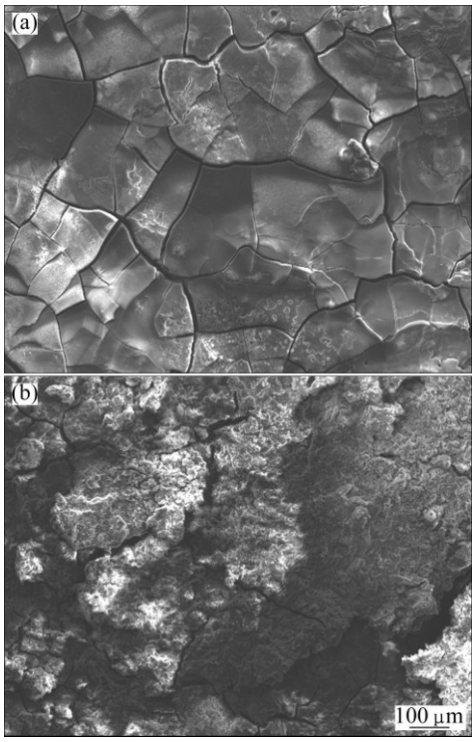

Fig. 5 Secondary electron images of surface morphologies after discharging at 180 mA/cm^2 for 600 s in 3.5% NaCl solution: (a) Mg−6%Al−5%Pb alloy; (b) Mg−9%Al−2.5%Pb alloy

3.4 Utilization efficiency

The utilization efficiency is important to an anode material. The calculated utilization efficiencies using Eq. (1) are summarized in Table 3. It can be observed that, at current densities of 10 mA/cm^2 and 180 mA/cm^2, the utilization efficiencies of Mg−9%Al−2.5%Pb alloy are both higher than those of Mg−6%Al−5%Pb alloy. Meanwhile, the utilization efficiencies for both alloys at a smaller current density are lower than those at a larger current density, which is in good agreement with several literatures [1,4].

The utilization efficiency can be influenced by the self-discharge reaction and the shedding of metallic particles. Firstly, as found above, the hydrogen evolution rate and corrosion current density of Mg−9%Al−2.5%Pb alloy are lower than those of Mg−6%Al−5%Pb alloy, thus leading to a weaker self-discharge reaction and an increase of utilization efficiency. Secondly, as shown in Fig. 6, the corroded surface of Mg−6%Al−5%Pb alloy after discharging at 180 mA/cm^2 in 3.5% NaCl solution for 1 h is uneven and has many holes, while the corroded surface of Mg−9%Al−2.5%Pb alloy is flat. These holes distributed in the corroded surface are caused by the shedding of some metallic particles during the process of discharge, and these detached metallic particles cannot be used to generate current via electrolytic dissolution. In addition, the generation of hydrogen bubbles preferentially took place inside the corrosion pores and therefore is detrimental to the anodic utilization efficiency [24]. Thus, Mg−9%Al−2.5%Pb alloy has a higher utilization efficiency and can serve as a good candidate for the anode material used in seawater activated battery.

Table 3 Utilization efficiencies of Mg−6%Al−5%Pb and Mg−9%Al−2.5%Pb alloys during galvanostatic discharge at different current densities

Alloy	Utilization efficiency, η/%	
	10 mA/cm^2	180 mA/cm^2
Mg−6%Al−5%Pb	42.6±0.4	76.1±0.8
Mg−9%Al−2.5%Pb	48.7±0.6	79.2±1.1

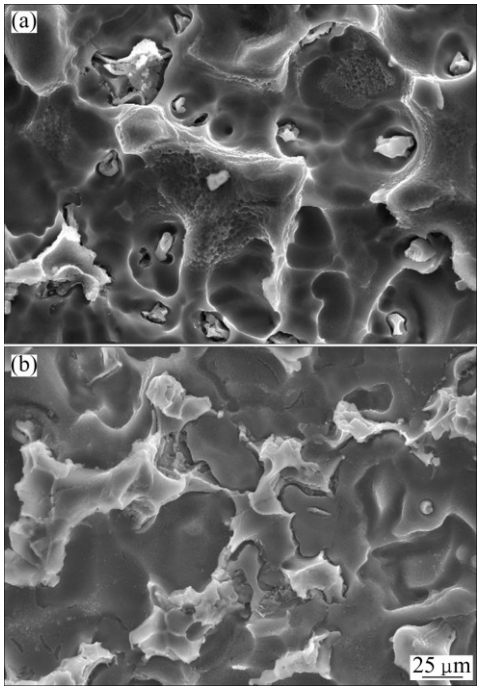

Fig. 6 Surface morphologies of magnesium alloys after discharging at 180 mA/cm^2 for 1 h in 3.5% NaCl solution after removing discharge products: (a) Mg−6%Al−5%Pb alloy; (b) Mg−9%Al−2.5%Pb alloy

3.5 Hydrogen evolution and mass loss data

Figure 7 presents the hydrogen evolution curves as a function of immersion time for the two alloys immersed in 3.5% NaCl solution. The slopes of curves represent the hydrogen evolution rate, which can determine the corrosion rate of magnesium alloy. As shown in Fig. 7, the corrosion rate of Mg−6%Al−5%Pb alloy is significantly higher than that of Mg−9%Al−2.5%Pb alloy. At the primary stage of immersion, the

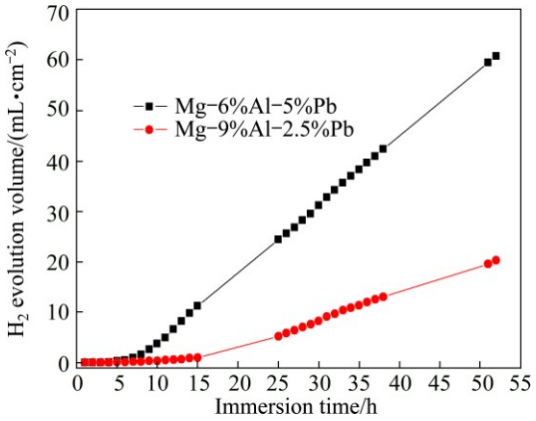

Fig. 7 Hydrogen evolution during immersion in 3.5% NaCl solution

hydrogen evolution rates of the two alloys are slow and the deviation is not obvious, indicating that there is incubation period at the primary stage of each corrosion. As the immersion time prolongs, the hydrogen evolution rates of the two alloys reach steady values, i.e., 1.3 mL/(cm^2·h) for Mg−6%Al−5%Pb alloy and 0.5 mL/(cm^2·h) for Mg−9%Al−2.5%Pb alloy. The mass loss data of these two alloys after immersion for 52 h in 3.5% NaCl solution can be obtained through calculation. The mass loss of Mg−6%Al−5%Pb alloy (67.8 mg/cm^2) after immersion for 52 h is obviously higher than that of Mg−9%Al−2.5%Pb alloy (16.7 mg/cm^2), revealing that the corrosion rate measured by mass loss is consistent with that obtained via hydrogen evolution and corrosion current densities.

It is found that the distribution of β-$Mg_{17}Al_{12}$ phase determines the corrosion resistance of Mg−Al alloys [25]. PARDO et al [26] and SONG and ATRENS [27] suggested that the β phase mainly served as a galvanic cathode and accelerated the corrosion process of the α-Mg matrix if the volume fraction of β phase was small; whereas for a high volume fraction, the β phase might act as an anodic barrier to inhibit the overall corrosion of the alloy. The β phase itself is more stable in NaCl solution and it has a lower corrosion rate. However, the cathodic hydrogen evolution on the β phase surface is significantly faster than that on the surface of the α-Mg matrix and thus the β phase is a more effective cathode [28]. According to the XRD patterns in Fig. 1 and the microstructure in Fig. 2, the volume fraction of β phase in Mg−9%Al−2.5%Pb alloy is higher than that in Mg−6%Al−5%Pb alloy, and this result well explains why the corrosion rate of Mg−9%Al−2.5%Pb alloy is slower than that of Mg−6%Al−5%Pb alloy. Figure 8 represents the

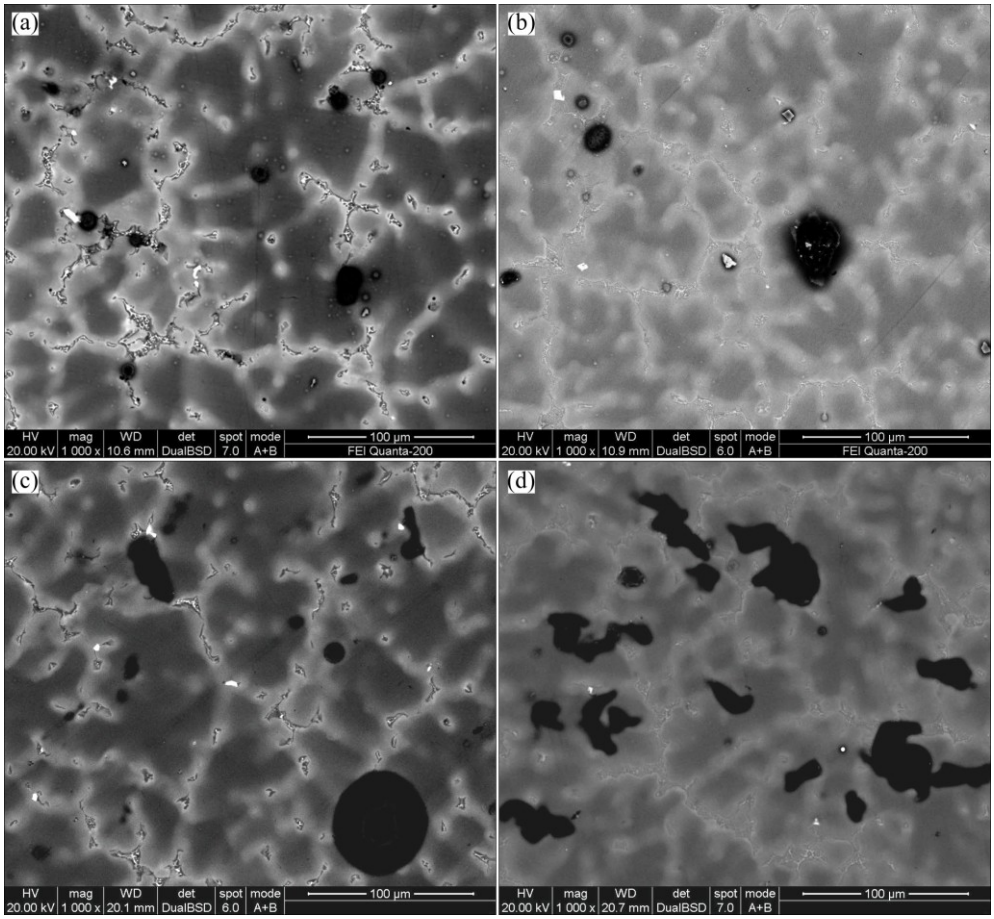

Fig. 8 Corrosion surface morphologies after immersion in 3.5% NaCl solution: (a) Mg−6%Al−5%Pb after 30 min; (b) Mg−9%Al−2.5%Pb after 30 min; (c) Mg−6%Al−5%Pb after 60 min; (d) Mg−9%Al−2.5%Pb after 60 min

corrosion surface morphologies of the two alloys after immersion for 30 min and 60 min in 3.5% NaCl solution. According to Figs. 8(a) and (c), the corrosion of Mg−6%Al−5%Pb alloy initiated from the β phase on the grain boundary, afterwards, gradually advanced by the dissolution of the α-Mg matrix adjacent to the region of the β-$Mg_{17}Al_{12}$ particles. While, the corrosion of Mg−9%Al−2.5%Pb alloy initiated from the α-Mg matrix, as indicated in Figs. 8(b) and (d). The corrosion section morphologies of the two alloys after immersion for 2 h in 3.5% NaCl solution are presented in Fig. 9. It can be found that the corrosion pits of Mg−6%Al−5%Pb alloy are large and deep (Fig. 9(a)), while the corrosion pits of Mg−9%Al−2.5%Pb alloy are small and shallow (Fig. 9(b)). The comparison of the these corrosion morphologies verifies the lower hydrogen evolution rate of Mg−9%Al−2.5%Pb alloy, and further explains the lower corrosion rate of Mg−9%Al−2.5%Pb alloy compared to Mg−6%Al−5%Pb alloy.

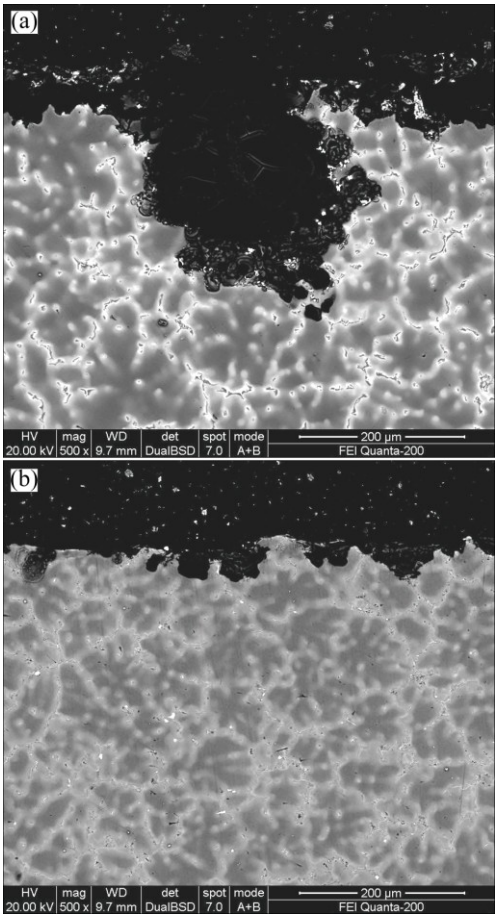

Fig. 9 Corrosion section morphologies after immersion for 2 h in 3.5% NaCl solution: (a) Mg−6%Al−5%Pb alloy; (b) Mg−9%Al−2.5%Pb alloy

4 Conclusions

1) Mg−9%Al−2.5%Pb alloy has lower self-corrosion rate than Mg−6%Al−5%Pb alloy, attributed to the increase of β-$Mg_{17}Al_{12}$ phase. In addition, the self-discharge reaction of Mg−9%Al−2.5%Pb alloy is suppressed and thus leads to a higher utilization efficiency than Mg−6%Al−5%Pb alloy.

2) The discharge activity of Mg−9%Al−2.5%Pb alloy is weakened because of the dense discharge products, which is caused by the reduction of Pb content. However, the debasing in the discharge activity for Mg−9%Al−2.5%Pb alloy is not obvious.

3) The Mg−9%Al−2.5%Pb alloy can serve as a good candidate for the anode material used in seawater activated battery in the condition of lower content of lead, which is harmful to the natural environment.

References

[1] WANG N G, WANG R C, PENG C Q, PENG B, FENG Y, HU C W. Discharge and corrosion performance of AP65 magnesium alloy in simulated seawater: Effect of temperature [J]. Journal of Materials Engineering and Performance, 2014, 23(12): 4374−4384.

[2] YU K, TAN X, HU Y N, CHEN F W, LI S J. Microstructure effects on the electrochemical corrosion properties of Mg−4.1%Ga−2.2%Hg alloy as the anode for seawater-activated batteries [J]. Corrosion Science, 2011, 53(5): 2035−2040.

[3] HASVOLD O, STORKERSEN N. Electrochemical power sources for unmanned underwater vehicles used in deep sea survey operations [J]. Journal of Power Sources, 2001, 96(1): 252−258.

[4] WANG N G, WANG R C, PENG C Q, FENG Y. Enhancement of the discharge performance of AP65 magnesium alloy anodes by hot extrusion [J]. Corrosion Science, 2014, 81: 85−95.

[5] BALASUBRAMANIAN R, VELUCHAMY A, VENKAAKRISHNAN N, GANGADHARAN R. Electrochemical characterization of magnesium/silver chloride battery [J]. Journal of Power Sources, 1995, 56(2): 197−206.

[6] WANG N G, WANG R C, PENG C Q, FENG Y, CHEN B. Effect of hot rolling and subsequent annealing on electrochemical discharge behavior of AP65 magnesium alloy as anode for seawater activated battery [J]. Corrosion Science, 2012, 64: 17−27.

[7] HASVOLD O, LIAN T, HAAKAAS E, STROKERSEN N, PERELMAN O, CORDIER S. CLIPPER: A long-range, autonomous underwater vehicle using magnesium fuel and oxygen from the sea [J]. Journal of Power Sources, 2004, 136(2): 232−239.

[8] UAHAYAN R, BHATT D P. On the corrosion behaviour of magnesium and its alloys using electrochemical techniques [J]. Journal of Power Sources, 1996, 63(1): 103−110.

[9] CAO D X, WU L, SUN Y, WANG G L, LV Y Z. Electrochemical behavior of Mg−Li, Mg−Li−Al and Mg−Li−Al−Ce in sodium chloride solution[J]. Journal of Power Sources, 2008, 177(2): 624−630.

[10] CAO D X, WU L, WANG G L, LV Y Z. Electrochemical oxidation behavior of Mg−Li−Al−Ce−Zn and Mg−Li−Al−Ce−Zn−Mn in sodium chloride solution [J]. Journal of Power Sources, 2008, 183(2): 799−804.

[11] LIN M C, TSAI C Y, Uan Y J. Electrochemical behaviour and corrosion performance of Mg−Li−Al−Zn anodes with high Al composition [J]. Corrosion Science, 2009, 51(10): 2463−2472.

[12] MA Y B, LI N, LI D Y, ZHANG M L, HUANG X M. Performance of Mg−14Li−1Al−0.1Ce as anode for Mg-air battery [J]. Journal of Power Sources, 2011, 196(4): 2346−2350.

[13] ZHAO M C, SCHMULZ P, BRUNNER S, LIU M, SONG G L, ATRENS A. An exploratory study of the corrosion of Mg alloys

during interrupted salt spray testing [J]. Corrosion Science, 2009, 51(6): 1277−92.
[14] FENG Yan, WANG Ri-chu, PENG Chao-qun, WANG Nai-guang. Influence of $Mg_{21}Ga_5Hg_3$ compound on electrochemical properties of Mg−5%Hg−5%Ga alloy [J]. Transactions Of Nonferrous Metals Society Of China, 2009, 19(1): 154−159.
[15] KOONTZ R F, LUCERO R D. Magnesium water-activated batteries [M]//Handbook of Batteries, New York: McGrraw-Hill. 2002, 17.11−17.27.
[16] SURESH K A R, MURALIDHARAN S, SARANGAPAIN K B, BALARAMACHANDRAN V, KAPALI V. Corrosion and anodic behaviour of zinc and its ternary alloys in alkaline battery electrolytes [J]. Journal of Power Sources, 1995, 57(1−2): 93−101.
[17] SONG G L, ATRENS A. Understanding magnesium corrosion—A framework for improved alloy performance [J]. Advanced Engineering Materials, 2003, 5(12): 837−858.
[18] SONG G L. Recent progress in corrosion and protection of magnesium alloys [J]. Advanced Engineering Materials, 2005, 7(7): 563−586.
[19] LIU W J, CAO F H, CHEN A N, CHANG L R, ZHANG J Q, CAO C A. Corrosion behaviour of AM60 magnesium alloys containing Ce or La under thin electrolyte layers. Part 1: Microstructural characterization and electrochemical behaviour [J]. Corrosion Science, 2010, 52(2): 627−638.
[20] SRINIVASAN A, PILLAI U T S, PAI B C. Effect of Pb addition on ageing behavior of AZ91 magnesium alloy [J]. Materials Science and Engineering A, 2007, 452−453(15): 87−92.
[21] BARBAGALLO S, LAUKLI H I, LOHNE O, CERRI E. Divorced eutectic in a HPDC magnesium–aluminum alloy [J]. Journal of Alloys and Compounds, 2004, 378(1−2): 226−232.
[22] WANG N G, WANG R C, PENG C Q, PENG B, FENG Y, HU C W. Discharge behaviour of Mg−Al−Pb and Mg−Al−Pb−In alloys as anodes for Mg-air battery [J]. Electrochimica Acta, 2014, 149(10): 193−205.
[23] WANG Nai-guang. Research on the electrochemical behavior of AP65 magnesium alloy in sodium chloride solution [D]. Changsha: Central South University, 2013. (in Chinese)
[24] SMOLJKO I, GUDIC S, KUZMANIC N, KLISKIC M. Electrochemical properties of aluminium anodes for Al/air batteries with aqueous sodium chloride electrolyte [J]. Journal of Applied Electrochemistry, 2012, 42(11): 969−977.
[25] ZENG Rong-chang, ZHANG Jin, HUANG Wei-jun, DIETZEL W, KAINER K U, BLAWERT C, KE Wei. Review of studies on corrosion of magnesium alloys [J]. Transactions of Nonferrous Metals Society Of China. 2006, 16(S2): s763−s771.
[26] PARDO A, MERINO M C, COY A E, ARRABAL R, VIEJO F, MATYLINA E. Corrosion behaviour of magnesium/aluminium alloys in 3.5wt.% NaCl [J]. Corrosion Science, 2008, 50(3): 823−834.
[27] SONG G L, ATRENS A. Corrosion mechanisms of magnesium alloys [J]. Advanced Engineering Materials, 1999, 1(1): 11−33.
[28] SONG G L, ATRENS A, DARGUSCH M. Influence of microstructure on the corrosion of diecast AZ91D [J]. Corrosion Science, 1999, 41(2): 249−273.

海水激活电池阳极材料用 Mg−9%Al−2.5%Pb 合金的腐蚀及放电性能

邓 敏，王日初，冯 艳，王乃光，王霖倩

中南大学 材料科学与工程学院，长沙 410083

摘 要：为了获得铅含量更低的 Mg−Al−Pb 合金阳极材料，采用浸泡实验及电化学测试技术研究了 Mg−9%Al−2.5%Pb(质量分数)合金的腐蚀及放电行为，并与 Mg−6%Al−5%Pb 合金进行比较。研究表明：与 Mg−6%Al−5%Pb 相比，更高的 Al 含量使得 Mg−9%Al−2.5%Pb 合金具有更低的自腐蚀速率及更高的阳极利用率；由于 Pb 含量降低，其放电活性有所减弱但仍能满足阳极材料的要求。因此，Mg−9%Al−2.5%Pb 合金有望作为海水激活电池阳极的备选材料，并且其具有更低的 Pb 含量。

关键词：Mg−Al−Pb 合金；阳极材料；自腐蚀速率；利用率；放电活性

(Edited by Yun-bin HE)